Opal and Inverse Opal Fabricated with a Flow-Controlled Vertical Deposition Method

Zuocheng Zhou and X. S. Zhao*

Department of Chemical and Biomolecular Engineering, National University of Singapore, 10 Kent Ridge Crescent, Singapore 119260

Received December 28, 2004. In Final Form: February 17, 2005

In this work, an improved vertical deposition method, namely, a flow-controlled vertical deposition (FCVD) method, was used to grow colloidal crystals with large spherical colloids in water solvent and to infiltrate the colloidal crystals. Using the FCVD method, latex spheres as large as 2 μm can be fabricated into colloidal crystals in water. In addition, the method works very well for controlling surface morphologies of silica-infiltrated opals. Furthermore, fabrication of colloidal crystal heterostructures was demonstrated.

Introduction

Three-dimensional (3D) photonic crystals have received a great deal of recent attention because of their technological application in photonics,[1,2] opotoelectronics,[3] data storage,[4] chemical and biochemical sensors,[5] and tissue engineering,[6] etc. Currently, there are two main fabrication strategies, namely, "top−down" microfabrication[7,8] and "bottom−up" self-assembly.[9] Although traditional microfabrication techniques offer a good control over structured defects, they are very time-consuming and expensive and have trouble in making 3D structures. The self-assembly approach, on contrast, affords 3D periodic structures in a controllable, simple, and inexpensive way. Thus, the past few years have seen remarkable advances in using self-assembly methods to create 3D photonic crystals.[9−12]

The self-assembly approach to 3D photonic crystals involves three steps. First, colloidal microspheres are organized into a colloidal crystal (also known as opal) via a self-assembly process. Second, a high refractive index material is infiltrated in the voids of the colloidal crystal. Third, the microspheres (template) are removed, leaving behind an ordered macroporous structure, namely, an inverse opal. The first step is extremely important in terms of fabrication of inverse opal with a full photonic band gap.[13,14] Up to now, several techniques have been successfully demonstrated for fabricating opals, such as confinement cell technique,[15] membrane filtration,[16] gravitational sedimentation,[17] and vertical deposition (VD).[18] Recently, we have described an improved VD method, namely, the flow-controlled vertical deposition (FCVD) method,[19] for fabrication of colloidal crystals of controllable and uniform thickness with colloidal microspheres as large as 1.5 μm. By control of the liquid-surface dropping velocity with a peristaltic pump, the problems of particle sedimentation and concentration gradients associated with traditional VD method can be minimized.

While growing colloidal crystals is important, complete infiltration of the voids of the colloidal crystal during the second step is also significant because the presence of a photonic band gap is closely related to the air volume fraction of the inverse opal.[20] On the other hand, control over the surface morphology of an infiltrated colloidal crystal is also of significance in many technological fields such as design and fabrication of plane defects,[12,21] synthesis of 3D−2D−3D hybrid structure,[22] and creation of surface patterning for subsequent nanofabrication.[23,24]

In this paper, the use of the FCVD method for fabrication of colloidal crystals with microspheres of diameters larger than 1.5 μm in water instead of ethanol and for infiltration of the colloidal crystals to obtain inverse opals with a controllable surface morphology is described.

Experimental Section

Reagents. The chemicals and solvents, including potassium persulfate (99%, Aldrich), sodium hydroxide pellets (99%, Merck), sodium dodecyl sulfates (99%, Aldrich), hydrochloric acid (37%, Merck), tetraethyl orthosilicate (TEOS, 98%, Acros Organics), ethanol (99.95%, Aldrich), and toluene (99.5%, Merck) were used as received. Styrene (99%, Aldrich) was washed four times with

* Corresponding author. Telephone: +65-68744727. Fax: +65-67791936. E-mail: chezxs@nus.edu.sg.

(1) Yablonovitch, E. *Phys. Rev. Lett.* **1987**, *58*, 2059.
(2) John, S. *Phys. Rev. Lett.* **1987**, *58*, 2486.
(3) Painter, O.; Lee, R. K.; Scherer, A.; Yariv, A.; O'Brien, J. D.; Dapkus, P. D.; Kim, I. *Science* **1999**, *284*, 1819.
(4) Cumpston, B. H.; Ananthavel, S. P.; Barlow, S.; Dyer, D. L.; Ehrlich, J. E.; Erskine, L. L.; Heikal, A. A.; Kuebler, S. M.; Lee, I.-Y. S.; McCord-Maughon, D.; Qin, J. Q.; Röckel, H.; Rumi, M.; Wu, X.-L.; Marder, S. R.; Perry, J. W. *Nature* **1999**, *398*, 51.
(5) Lee, K.; Asher, S. A. *J. Am. Chem. Soc.* **2000**, *122*, 9534.
(6) Kotov, N. A.; Liu, Y.; Wang, S.; Cumming, C.; Eghtedari, M.; Vargas, G.; Motamedi, M.; Nichols, J.; Cortiella, J. *Langmuir* **2004**, *20*, 7887.
(7) Yablonovitch, E.; Gmitter, T. J.; Leung, K. M. *Phys. Rev. Lett.* **1991**, *67*, 2295.
(8) Aoki, K.; Miyazaki, H. T.; Hirayama, H.; Inoshita, K.; Baba, T.; Sakoda K.; Shinya, N.; Aoyagi, Y. *Nat. Mater.* **2003**, *2*, 117.
(9) López C. *Adv. Mater.* **2003**, *15*, 1679.
(10) Arsenault, A.; Fournier-Bidoz, S.; Hatton, B.; Míguez, H.; Tétreault, N.; Vekris, E.; Wong, S.; Yang, S. M.; Kitaev, V.; Ozin, G. A. *J. Mater. Chem*. **2004**, *14*, 781.
(11) Norris, D. J.; Arlinghaus, E. G.; Meng, L.; Heiny, R.; Scriven, L. E. *Adv. Mater*. **2004**, 16, 1393.
(12) Tétreault, N.; Mihi, A.; Míguez, H.; Rodríguez, I.; Ozin, G. A.; Meseguer, F.; Kitaev, V. *Adv. Mater.* **2004**, *16*, 346.
(13) Vlasov, Y. A.; Bo, X.-Z.; Sturm, J. C.; Norris, D. J. *Nature* **2001**, *414*, 289.
(14) Blanco, A.; Chomski, E.; Grabtchak, S.; Ibisate, M.; John, S.; Leonard, S. W.; López, C.; Meseguer, F.; Míguez, H.; Mondia, J. P.; Ozin, G. A.; Toader, O.; van Driel, H. M. *Nature* **2000**, *405*, 437.
(15) Park, S. H.; Qin, D.; Xia, Y. *Adv. Mater.* **1998**, *10*, 1028.
(16) Velev, O. D.; Jede, T. A.; Lobo, R. F.; Lenhoff, A. M. *Nature* **1997**, *389*, 447.
(17) Van Blaaderen, A.; Ruel, R.; Wiltzius, P. *Nature* **1997**, *385*, 321.
(18) Jiang, P.; Bertone, J. F.; Hwang, K. S.; Colvin, V. L. *Chem. Mater.* **1999**, *11*, 2132.
(19) Zhou, Z.; Zhao, X. S. *Langmuir* **2004**, *20*, 1524.
(20) Busch, K.; John, S. *Phys. Rev. E* **1998**, *58*, 3896.
(21) Palacios-Lidón, E.; Galisteo-lópez, J. F.; Juárez, B. H.; López, C. *Adv. Mater.* **2004**, *16*, 341.
(22) Chutinan, A.; John S. *Photonics Nanostruct.* **2004**, *2*, 41.
(23) Lee, W.; Jin, M.-K.; Yoo, W.-C.; Lee, J.-K. *Langmuir* **2004**, *20*, 7665.
(24) Jiang P. *Angew. Chem., Int. Ed*. **2004**, *43*, 5625.

10.1021/la046775t CCC: $30.25
Published on Web 03/26/2005

10 wt % NaOH solution, followed by another four times with deioned water before use.

Synthesis of Polystyrene (PS) Microspheres. PS microspheres with diameters of 0.44, 0.58, 0.8, 1, and 2 μm and a standard deviation of less than 5% were synthesized using an emulsifier-free emulsion polymerization method.[25] The as-prepared mother emulsion of PS latex spheres was diluted to a certain volume fraction before use (a value of 1.05 g/mL was taken as the density of the PS microspheres).

Fabrication of Opals with a FCVD Method. The growth of colloidal crystals from PS colloids in water was carried out at 30 °C using the FCVD method as described elsewhere.[19] In brief, a glass substrate was vertically fixed in a vessel containing a PS colloidal suspension. The liquid container was connected with a peristaltic pump, which was used to control the liquid surface dropping velocity of the colloidal suspension. Thus, the deposition rate of the colloidal particles can be controlled because self-assembly of colloids is driven by the capillary force imposed by the meniscus at the air−liquid interface.

Fabrication of Silica Inverse Opals. After the colloidal crystal obtained above was annealed at 105 °C for 10 min, it was fixed vertically in the vessel of the FCVD setup. A SiO_2 sol precursor, which was prepared by mixing tetraethyl orthosilicate (TEOS), ethanol, and 0.1 M HCl solution with volume ratio of 1:6:0.1, was poured into the vessel with or without a cap. Then the silica solution was withdrawn using the peristaltic pump at a constant flow rate (0.5, 1, 2, and 5 μm/s). After the precursor solution was completely withdrawn, the silica-infiltrated colloidal crystal was dried at room temperature. The infiltration process was repeated to increase infiltration. An inversed SiO_2 opal was obtained after removal of the PS spheres by soaking in toluene at 60 °C for 24 h or calcination at 500 °C for 5 h.

Fabrication of an Opal Heterostructure. The experimental process was similar to that of the fabrication of opals except that an infiltrated opal was used as a substrate.

Characterization. The morphologies of the colloidal crystals and inverse opals were imaged with a JEOL JSM-6700F scanning electron microscope (SEM) operating at 10 kV. A sample was dispersed on a conductive carbon tape attached to a copper mount and coated with Pt. The optical reflectance spectra were obtained on a Shimadzu UV-3101PC UV−visible−near-infrared spectrophotometer. A homemade mask was used to constrain the incident light into a 5 mm diameter circle.

Results and Discussion

Fabrication of Large Colloidal Spheres into Colloidal Crystals in Water. The use of water as a solvent is practically significant because (1) water does not have a swelling effect on PS spheres so that the colloidal suspension can be recycled and reused, (2) water is a readily available and environmentally friendly solvent, and (3) water has a higher density and a larger surface tension than that of ethanol, thus large colloidal particles can be used without provoking remarkable particle sedimentation and concentration gradient. Figure 1 shows the SEM images of colloidal crystals fabricated from PS spheres in water with diameters of 1 and 2 μm, respectively. It can be seen that the colloidal crystals all display a uniform thickness. In addition, compared with the PS−ethanol system described previously,[19] the colloidal crystals fabricated in a PS−water system with 1 μm PS spheres have more layers under otherwise identical conditions (eight layers in water and four layers in ethanol). This can be understood with the help of the following formula

$$k = \frac{\beta L}{0.605} \frac{j_e \varphi}{d(V_p + j_e)(1 - \varphi)} \quad (1)$$

where k is the layer number, β is a constant depending on particle−particle and particle-substrate interactions,

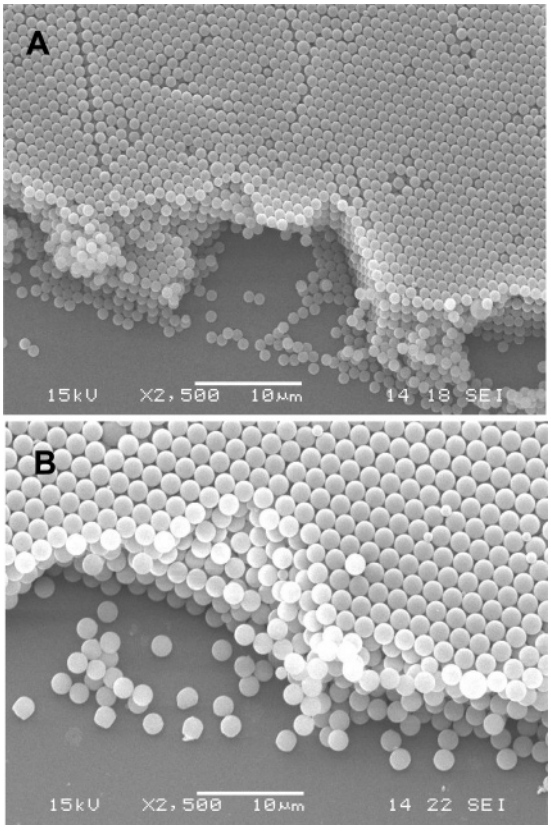

Figure 1. Colloidal crystals fabricated by the FCVD method from the PS−water system with a volume fraction of 1% at 30 °C. (A) The diameter of the PS spheres was 1 μm, and the liquid surface dropping velocity was 0.26 μm/s. (B) The diameter of the spheres was 2 μm, and the liquid surface dropping velocity was 1.6 μm/s.

L is the meniscus height, j_e is the evaporation rate of the solvent, d is the particle diameter, φ is the particle volume fraction of the colloidal suspension, and V_P is the liquid-surface dropping velocity induced by the pump. Apparently, k will decrease if water is used as a solvent because the evaporation rate of water is slower than that of ethanol under otherwise identical conditions. The evaporation rates of ethanol and water measured under our experimental conditions are about 0.31 and 0.13 μm/s, respectively. As a result, if only the factor of solvent evaporation is considered, replacing ethanol with water will result in a decrease in the number of layers of a factor of about 0.42.

However, according to eq 1 k is dependent upon L as well, which is determined by the surface tension of the colloidal suspension.[18,26] Although the surface tension is an important factor which affects the thickness of colloidal crystals in vertical deposition method, only a few studies have been conducted on this factor. Marquez and Grady[27] studied the roles of spreading agents (i.e., sodium dodecyl sulfates (SDS), polyacrylamide, and octylphenoxy poly(ethyleneoxy)ethanol) in the formation of 2D arrays of latex spheres via the Langmuir−Blodgett technique. Here we used surfactant SDS to change the surface tension of PS−water suspensions to determine the effect of surface tension on k. In the research of Marquez and Grady,[27] to form ordered 2D array high concentrations of SDS (34.7−52.1 mM) are used, which are much higher than the critical micelle concentration (cmc) of SDS (8.3 mM). However, when such a high concentration of SDS was used in

(25) Shim, S.-E.; Cha, Y.-J.; Byun, J.-M.; Choe, S. *J. Appl. Polym. Sci.* **1999**, *71*, 2259.

(26) Zhou, Z.; Zhao, X. S., Zeng, X. T. *Surf. Coat. Technol.*, in press.

(27) Marquez, M.; Grady, B. P. *Langmuir* **2004**, *20*, 10998.

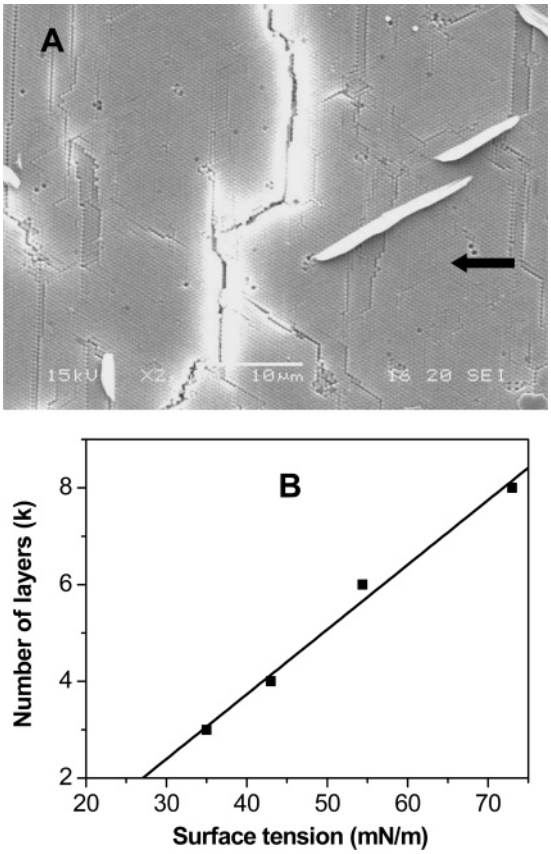

Figure 2. (A) Colloidal crystal fabricated with a SDS concentration of 10 mM. (B) Number of colloid layers versus surface tension ($d = 1$ μm, $V_P = 0.26$ μm/s).

fabricating colloidal crystals, the clusters of SDS were formed during the experiment as indicated by the arrow in Figure 2A, which could destroy the periodicity and surface morphology of the colloidal crystals. In addition, the surface tension of the water will not decrease further when the concentration of the SDS is higher than the cmc. Therefore, in our experiment the highest concentration of SDS was cmc 8.3 mM. The experimental number of colloidal crystal layers against surface tension is plotted in Figure 2B. It is seen that the number of layers is proportional to the surface tension of the suspension. With this experimental results, we can evaluate the effects of solvents, water and ethanol, more precisely. The surface tension of ethanol is about 22.2 mN/m. Extrapolated from the plot of Figure 2B, the number of the layers of the colloidal crystal is 1.35 when the surface tension is 22.2 mN/m. Because the colloidal crystal fabricated with pure water as solvent has eight layers, by replacing water with ethanol, the number of layers can be decreased to about 5.9 times if only the effect of surface tension is considered. When both effects of solvent evaporation rate and surface tension on the number of colloidal layers are considered, it can be estimated that the use of water as a solvent can produce a thicker colloidal crystal film than that of ethanol under otherwise identical conditions (about 2.5 times thicker), which is almost consistent with the experimental result (2 times).

Previously, it has been shown that with ethanol as a solvent the largest size of PS colloidal spheres that can be assembled into colloidal crystals is about 1.5 μm.[19] This limitation is mainly due to the relatively fast sedimentation of PS spheres in ethanol. In this work, when water was used as the solvent, it can be seen from Figure 1B that PS spheres as large as 2 μm can be fabricated into colloidal crystals. According to Stokes law, both the viscosity and the density of the solvent in a colloidal system affect the sedimentation velocity of the colloidal particles. Because at 30 °C the density of water (0.996 g/mL) is larger than that of ethanol (0.781 g/mL) while its viscosity (0.00797 g/(cm/s)) is slightly lower than that of ethanol (0.0101 g/(cm/s)), PS spheres deposit at a slower rate in water than in ethanol. In other words, it becomes more efficient to grow colloidal crystals in water than in ethanol.

FCVD Method for Fabrication of Inverse Opals. To demonstrate the use of the FCVD method for infiltration of opals, a silica precursor was used because silica can be easily processed and integrated with the current electronic devices such as silicon-on-insulator. In addition, the transparence of silica in the visible and near-IR ranges makes it suitable for optical communication applications.[21]

Actually, the FCVD setup was developed on the basis of the Langmuir-Blogett (LB) method. As a result, it is, to some extent, similar to the dipping method.[28−30] However, our FCVD method has a number of advantages over the dipping method. First, the dropping of the liquid surface was controlled with the help of a peristaltic pump, not involving any complex facilities such as motor and controller compared with the dipping method. Second, because the substrate is fixed in the colloidal suspension, the shaking problem during lift-up of the substrate can be avoided. Third, in the FCVD method, the dropping velocity of the liquid surface can be determined by both the pumping flow rate and the cross area of the container.[19] As a result, the dropping velocity of the liquid surface can be precisely controlled. In addition, as the substrate was fixed in the container, several samples can be prepared at the same time. Thus the FCVD infiltration can be much more efficient than the dipping method.

Figure 3A shows the SEM images of PS colloidal crystal after one-time infiltration of silica. It can be seen that the crystal was filled with silica uniformly and the ordered structure was intact during infiltration, suggesting the feasibility of the FCVD method for infiltration of opals. In the course of the infiltration process, the precursor solution moved vertically, which prevented the coagulation of the precursor on the surface of the colloidal crystals. Another observation from Figure 3A is the ordered silica pattern formed on the region of the glass substrate where PS spheres were stripped off. The pattern was formed between the bottom layer of PS spheres and the substrate because of a better compatibility of the glass substrate with TEOS than with PS spheres.

The optical reflectance spectra of the colloidal crystal and the silica-infiltrated composites are shown in Figure 3B. Because the diameter of the PS spheres is known, Bragg's law combined with Snell's law in eq 2 can be used to calculate the position of the reflectance peak of the colloidal crystal fabricated from the PS spheres[31]

$$\lambda_{max} = 2d(n_a^2 - \sin^2\theta)^{1/2} \quad (2)$$

where λ_{max} is the wavelength of the peak, d is the lattice constant, n_a is the average refractive index of the materials, and θ is the angle between the incident light and the surface normal of the sample. As the surface of our samples

(28) Ye, Y.-H.; Badilescu, S.; Truong, V.-V. *Appl. Phys. Lett.* **2002**, *81*, 616.
(29) Kuai, S.; Badilescu, S.; Bader, G.; Brüning, R.; Hu, X.; Truong, V.-V. *Adv. Mater.* **2003**, *15*, 73.
(30) Kuai, S. L.; Hu, X. F.; Truong, V.-V. *J. Cryst. Growth* **2003**, *259*, 404.
(31) Schroden, R. C.; Al-Daous, M.; Blanford, C. F.; Stein, A. *Chem. Mater.* **2002**, *14*, 3305.

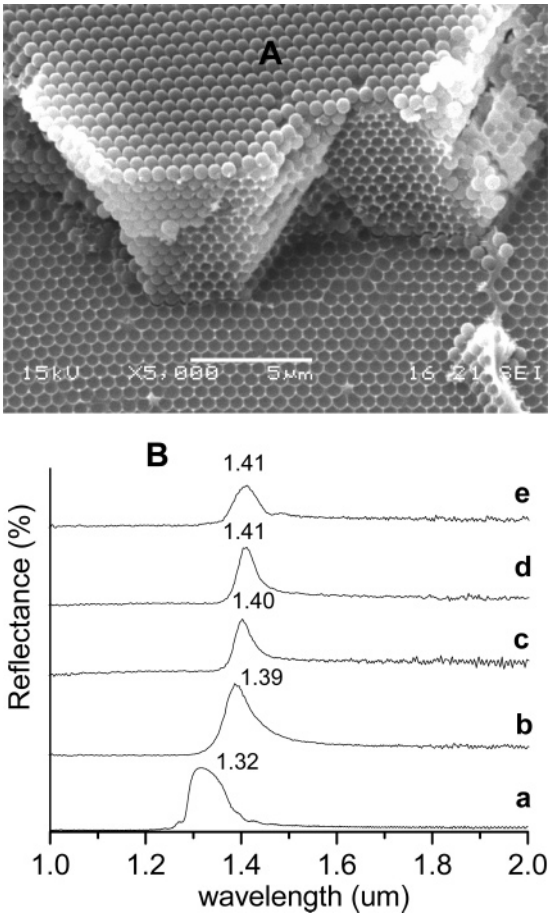

Figure 3. (A) SEM image of PS colloidal crystal after one infiltration with silica using the FCVD method. (B) Optical reflectance spectra of a colloidal crystal fabricated with PS spheres of 0.58 μm in diameter after annealing (a) and after infiltration with silica for one (b), two (c), three (d), and four times (e).

is predominated by (111) face, the lattice constant can be calculated with eq 3

$$d = d_{111} = (2/3)^{1/2}D \tag{3}$$

where D is the diameter of the PS spheres. The average effective refractive index of the structure is related to the volume fractions of PS and silica that can be obtained from eq 4[31]

$$n_a = n_{PS}f_{PS} + n_{silica}f_{silica} + n_{air}f_{air} \tag{4}$$

where f is the volume fraction of the compositional materials. The refractive indexes of the PS, silica, and air were taken as 1.59, 1.44, and 1, respectively. The calculation showed that the reflectance spectra of the bare opal should be at about 1.36 μm, which is in good agreement with the experimental result 1.32 μm (In bare opal, the volume fraction of the PS and air is taken as 74% and 26%, respectively.). The slight difference is due to particle shrinkage during the annealing process. Nevertheless, the experimental value, 1.32 μm, was used to estimate the actual sphere size in the infiltrated colloidal crystals, which is 0.56 μm. It was obtained that after infiltration for four times the positions of the reflectance peak were at 1.41 μm. The calculated value 1.42 μm is very close to the measured value of the sample after infiltration four times, indicating a complete infiltration of the colloidal crystals. Although the other three infiltrated samples all display a peak at the wavelength position less than 1.42 μm, the differences are insignificant, indicating that the FCVD method is highly efficient for infiltration of opals.

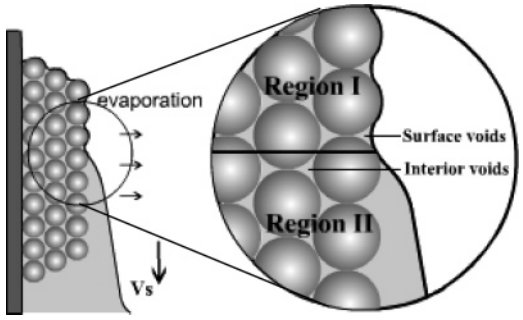

Figure 4. An illustration of the FCVD method for infiltration of opal.

The process of using the FCVD system for infiltration of opals with a silica precursor is illustrated in Figure 4. Shortly after soaking of the colloidal film into the silica precursor solution, the voids among the PS spheres are filled with the solution completely due to the strong capillary force induced by the small voids. In the meantime, a wedge-shaped thin liquid film is formed on the surface of the colloidal crystal induced by evaporation-induced force, capillary force, and gravity.[32] Evaporation of the solvent from this liquid film leads to a gradual concentrating of the silica inorganic species, resulting in an increase in viscosity. With continuous lowering down of the liquid surface, the liquid film moves down as well. Therefore, the top part of the colloidal crystal film emerges from the liquid solution as shown in region I of Figure 4. However, in this area the solution can still hold in both the interior and surface voids of the colloidal crystal due to capillary force and increased viscosity. With further evaporation of the solvent, gelation of silica sol takes place. In our experiments, due to the low concentrations of TEOS used (14 vol %), considerable shrinkage of the infiltrated silica material occurred, resulting in vacancies in the voids. However, as long as the colloidal crystal is partially immersed in the precursor solution, the liquid can take over the vacancies due to capillary force. Such a process continues until there is no more contact between the colloidal crystal and the precursor solution. As a result, despite the low concentration of silica sol used, a high infiltration ratio was obtained. This discussion is supported by the reflectance spectra shown in Figure 3B, which shows that with only a one time infiltration the peak position, 1.39 μm, is close to that of the completely infiltrated sample, 1.42 μm, indicating a high infiltration ratio.

In our experiment, we also carried out the experiments that with different liquid surface dropping velocity from 0.5 to 5 μm/s. The peak positions and the infiltration ratios of the silica after one infiltration, which are calculated from eqs 2, 3, and 4, are listed in Table 1. It can be found that with the increase of the velocity, the infiltration ratios are decreased. It can be concluded that a long contact time between the colloidal crystal and the silica solution can lead to a high infiltration ratio. Therefore, a slow liquid surface dropping velocity is important to enhance the infiltration ratio.

FCVD Method for Surface Patterning. To obtain uniform surface morphology of an infiltrated opal, the chemical vapor deposition (CVD) method has been successfully employed.[12,21,33] However, the CVD method

(32) Brinker, C. J.; Hurd, A. J. In *Sol–gel Science and Technology*; Pope, E. J. A., Sakka, S., Klein L. C., Eds.; The American Ceramic Society Press: Westerville, OH, 1995; Vol. 55, p 157.

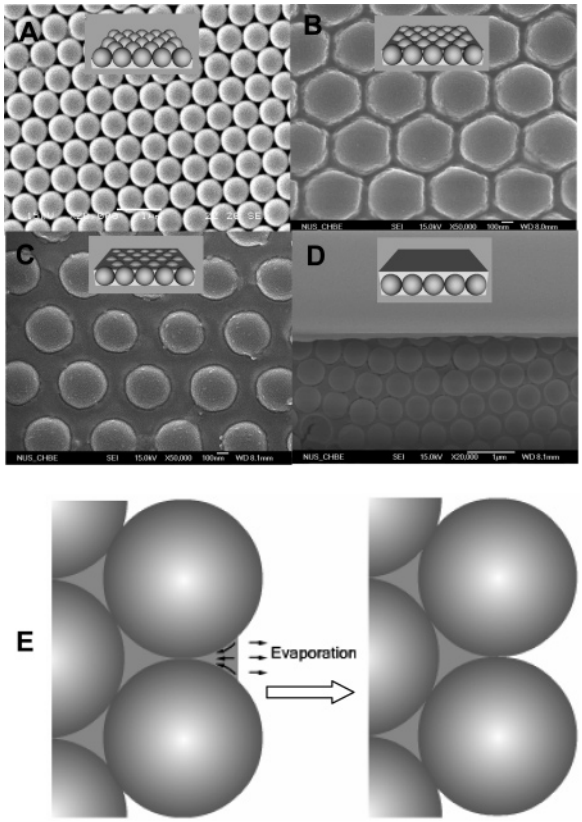

Figure 5. SEM images of side and top views of silica inverse opals with (A) one, (B) three, and (C) four infiltrations. The inset in (B) is an enlarged image.

Table 1. Reflectance Peak Positions and Volume Fractions of Silica for Infiltrated Opals with Different Surface Dropping Velocities[a]

liquid surface dropping velocity (μm/s)	reflactance peak position (μm)	volume fraction of silica (%)
0.5	1.40	21.6
1	1.39	19.2
2	1.37	14.2
5	1.34	6.70

[a] The volume fraction of PS spheres was taken as 74%.

involves special precursors such as $SiCl_4$. In this work, we also attempted to use the FCVD method to control surface morphology and patterning of infiltrated opals.

Figure 5A−D shows the top views of PS colloidal crystals after infiltration of silica with different times, together with schematic illustrations of side views. It is seen that after one infiltration, the surface morphology is the same to that of the PS colloidal crystal (see Figure 1). After three infiltrations, it is clearly seen that the interstitials among the spheres are fully filled (see Figure 5B). After four infiltrations (see Figure 5C), the PS spheres are seen as separated islands embedded in a silica matrix. With eight infiltrations, a smooth silica layer on the surface of the colloidal crystal formed (see Figure 5D). With the help of the inset illustrations it can be understood that silica was growing from the bottom to the top of the colloidal crystal film with increasing infiltration cycles. However, the reflectance spectra in Figure 3B demonstrate that after one infiltration the colloidal crystal are almost fully filled with silica. Thus, it can be concluded that the "bottom-up" growing model is applicable to the top layer only. As shown in area I of Figure 4, after the colloidal crystal leaves the liquid phase, there still has precursor solution holding in the surface voids. However, no silica is found on the surface of the colloidal crystal after the sample was dried (see Figure 5A). The possible explanation for the disappearance of the solution in the surface voids is illustrated in Figure 5E. On one hand, the solvent in the surface voids will evaporate away, which leads to the shrinkage of the volume of the solution. On the other hand, the shrinkage happens to the precursor solution in the interior voids as well. As discussed above, when the colloidal crystal leaves the liquid completely, no more supplements can be obtained from the solution. As a result, there will be vacancies formed in the interior voids and the precursor in the surface voids will be sucked into these vacancies. With more infiltration cycles, the interior voids can be fully filled. Under such a circumstance, the precursor solution in the surface voids can be intact (see panels B and C of Figure 5). With further infiltration, the surface voids are fully filled to form a silica layer on the surface of the colloidal crystal. As a result, by manipulation of infiltration cycles, the surface morphology can be precisely controlled from an opal-like surface to a uniform silica layer.

After removal of the PS spheres of the infiltrated colloidal crystals with toluene, ordered macroporous silica films are obtained. Shown in Figure 6 are the SEM images of the silica films prepared with one, three, and four infiltrations of silica viewed from different faces. It can be seen that the surfaces of the films are uniform and smooth. These SEM images also reveal that increasing infiltration cycles increased the solid volume fraction. The optical reflectance spectra (see Figure S1 in Supporting Information) also confirmed this conclusion.

When infiltration was carried out using the FCVD setup without a cap to cover the vessel, an inverse opal with an interesting surface morphology was obtained as can be seen from Figure 7 (the SEM images in lower magnifications are shown in Figure S2 in Supporting Information). A silica ring is seen between two air holes as indicated by the arrows in panels A and B of Figure 7. The locations of these rings are just the places where two PS spheres were connected in the colloidal crystal template. However, such rings are only seen on the surface but not in the interior. Further experimental results showed that the formation of such ring structures is independent of template removal methods (calcinations or solvent etching). It is believed that the formation of the ringlike structure is related to hydrolysis and drying conditions. When the colloidal crystal moves out from the precursor solution as illustrated in Figure 4, the colloidal crystal holds the precursor in both the surface voids and the interior voids of region I. In an open system, the hydrolysis and condensation of TEOS take place faster than in a closed system because ethanol is released more efficiently and the precursor contacts with air directly. Because the corner around the contact point of two neighboring spheres has a very small contact angle, the concentrated precursor solution will congregate at the corner due to strong capillary force as illustrated in Figure 8. In addition, in the open system, the precursor solution in the surface voids solidifies much faster than that in the interior voids. In other words, the interior voids are fully filled with the precursor solution during the solidification of the precursor in the surface voids, preventing sucking of the precursor solution from the surface voids to the interior voids. Thus when the precursor solidifies completely, the silica rings will form at these sites as can be seen from Figure 7C. The

(33) Míguez, H.; Tétreault, N.; Hatton, B.; Yang S. M.; Perovic D.; Ozin, G. A. *Chem. Commun.* **2002**, 2736.

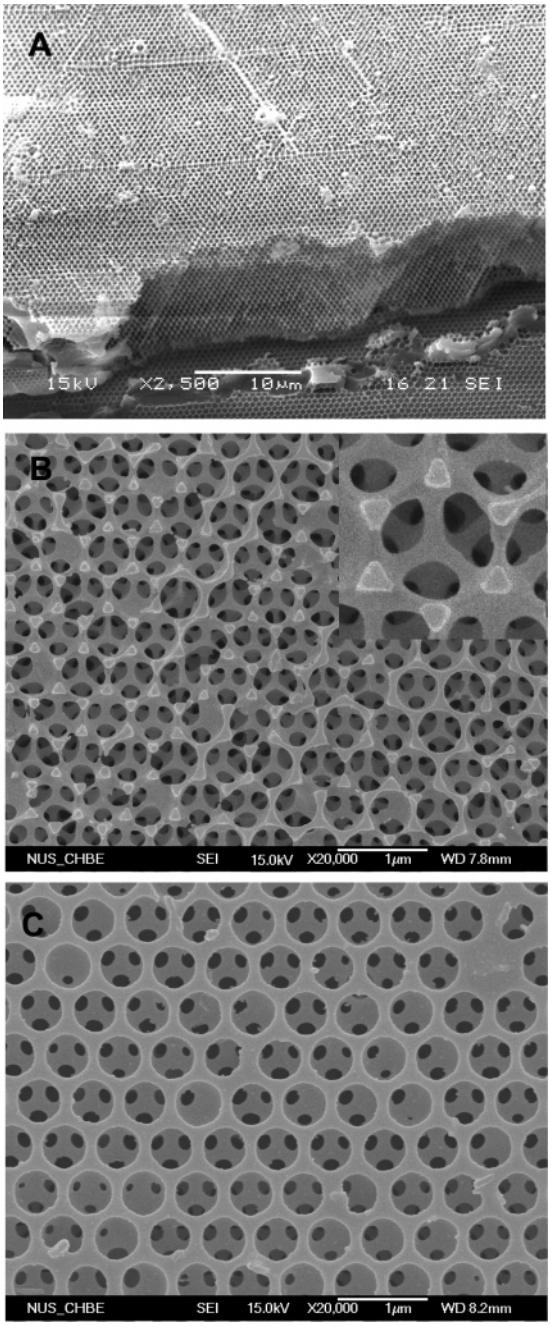

Figure 6. SEM images of the surface morphologies of PS colloidal crystals after different times of silica infiltration: (A) one, (B) three, (C) four, and (D) eight times. The insets are side view illustrations.

area enclosed by three PS spheres is triangular in shape as illustrated in Figure 8B, that can be observed from Figure 7A. Shown in Figure 7D is an enlarged SEM image of the patterned surface viewed along (100) face. As indicated by the arrows, in addition to a ring, a double-layered shell can also be seen. The formation mechanism of these two structures can be explained with the enlarged illustrations in Figure 8. Because the corner around the contact point of two neighboring spheres is formed by two spherical surfaces, the distance between these two surfaces increases from the contacted point to the outer space. As a result, if the amount of the precursor is not enough, it can only fill in the inner part of the corner and appear as single layer. However, if more silica is available, it will grow along the spherical surfaces and a double-layer shell will be obtained due to the increased distance.

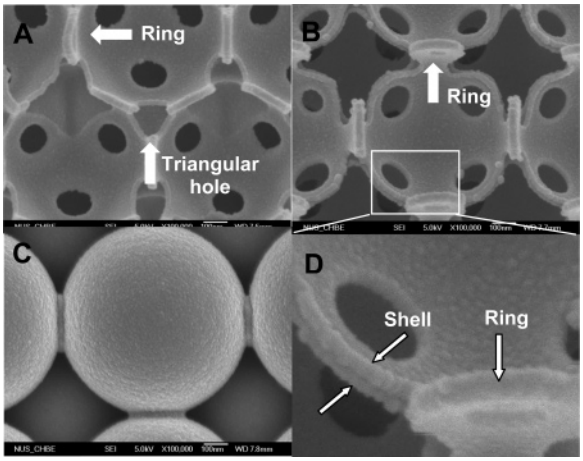

Figure 7. SEM image of an inverse opal with a ringlike surface morphology viewed from (A) [111] and (B) [100] faces, respectively. (C) SEM image of silica-infiltrated opal. (D) SEM image of (A) at a larger magnification.

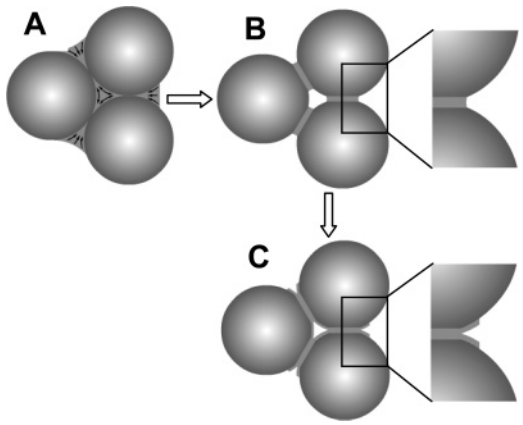

Figure 8. An illustration of the formation process of surface silica rings.

Fabrication of Colloidal Crystal Heterostructure. Use of the infiltrated colloidal crystal as a substrate for subsequent growth of a second layer with the FCVD method was attempted. Figure S3A shows the SEM image of PS spheres of 0.44 μm grown on a silica-infiltrated colloidal crystal of PS sphere with a diameter of 0.58 μm. It can be seen that the spheres in the top layer were arranged without disturbing the periodicity of the bottom layer. The presence of two optical reflectance peaks (see Figure S3B) indicates that the sample is a heterogeneous structure. The experimental peak positions are consistent with the calculated values, namely, 1.03 and 1.40 μm, respectively.

Conclusions

The flow-controlled vertical deposition (FCVD) method reported previously[17] can be used to fabricate opals with large diameters in water solvent and to infiltrate the opals. In comparison with alcohol solvent, water solvent allows PS spheres as large as 2 μm in diameter to be fabricated into opals. With the FCVD method and using silica infiltration as an example, complete infiltration of the voids of the opals can be achieved. In addition, the surface morphology of inverse opals can be precisely controlled. Furthermore, heterostructured colloidal crystals with more than one optical reflectance peak can be fabricated using the FCVD method.

Acknowledgment. We thank the Agency for Science, Technology and Research (A*STAR) of Singapore for financial support.

Supporting Information Available: Optical reflectance spectra of inverse silica opals, SEM image of silica rings on inversed silica surface, and SEM and reflectance spectrum of a colloidal crystal heterostructure. This material is available free of charge via the Internet at http://pubs.acs.org.

LA046775T